Desalination and Water Treatment
www.deswater.com

doi: 10.5004/dwt.2021.27456

230 (2021) 259–267
August

Performance of photocatalytic ceramic membrane for hospital effluent treatment

Watsa Khongnakorn[a,*], Phudis Pattanasattayavong[a], Kathayut Tanthai[a], Panitan Jutaporn[b]

[a]*Center of Excellence in Membrane Science and Technology, Department of Civil and Environmental Engineering, Faculty of Engineering, Prince of Songkla University, Hat Yai, Songkhla, 90110, Thailand, Tel. +66 74287122; Fax: +66 74459396; email: watsa.k@psu.ac.th (W. Khongnakorn), Tel. +66 74287015; Fax: +66 74459396; email: phudis.pat@gmail.com (P. Pattanasattayavong), Tel. +66 74287016; Fax: +66 74459396; email: kathayut9227@gmail.com (K. Tanthai)*

[b]*Department of Environmental Engineering, Faculty of Engineering, and Research Center for Environmental and Hazardous Substance Management, Khon Kaen University, Khon Kaen, 40002, Thailand, Tel. +66 610245666; email: panitju@kku.ac.th*

Received 28 February 2021; Accepted 19 May 2021

ABSTRACT

This study aims to investigate the effect of binder used in dip-coating techniques on ceramic photocatalytic membrane reactor (PMR) and to evaluate the performance of the PMR in the treatment of secondary effluent from two hospitals. The catalytic membrane was dipped and coated with TiO_2, then either sodium lauryl sulfate (SLS) or polyethylene glycol (PEG) was used as binders. The photocatalytic membranes were characterized using scanning electron microscopy and X-ray diffraction. Organic matter in the wastewater effluent was measured and characterized using chemical oxygen demand, dissolved organic carbon (DOC), and fluorescent excitation-emission matrix (EEM). DOC removal efficiencies of the PMR experiments using the TiO_2-PEG and the TiO_2-SLS membranes were 20.0% and 28.5%, respectively. EEM characterization revealed four fractions of organic matter were presented in the system, namely tyrosine-like, tryptophan-like, humic-like and fulvic-like organic matter. The TiO_2-assisted PMR had preferential removal of protein-like dissolved organic matter (DOM) over humic-like substances, as protein-like DOM was preferably oxidized by hydroxyl radicals in the reactor.

Keywords: Photocatalytic membrane reactor; Ceramic membrane; Dissolved organic carbon; Fluorescent spectroscopy; Hospital effluent

1. Introduction

The photocatalytic process is environmentally friendly with a number of advantages compared to some alternative technologies. Many researchers have been studied the application for hardly biodegradation compound in water and wastewater such as synthetic azo dye [1], azo dye (Acid Orange) [2], oily wastewater [3], humic acid [4,5], carbaryl [6], antibiotic pharmaceutical [7], micropollutant [8], etc. The well-known catalysts are metal oxide such as titanium (TiO_2), zinc (ZnO), zirconium (ZrO_2), hematite (Fe_2O_3). Titanium dioxide (TiO_2) has been previously used as a catalyst to remove organic pollutants for its economic cost, practical and eco-friendly products [9]. The photocatalytic membrane reactor (PMR) is the process that combines membrane filtration and photocatalysis in the same reactor. There are two types of photocatalytic membranes, which are (i) polymeric membrane and (ii) ceramic membrane. The ceramic membrane was commonly used for its high temperature and chemical resistance, high water flux, and stability during operation [7,10].

Al_2O_3 based ceramic membrane was studied for macroporous supports that immobilize photocatalysts for membrane photocatalytic processing according to the composition of the hydroxy group that increased hydrophilicity of the membrane [2,11]. Sol dip-coating technique is widely used for coating the TiO_2 on a ceramic membrane. Zhang et al. [12] have studied the preparation of TiO_2/Al_2O_3 composite

* Corresponding author.

1944-3994/1944-3986 © 2021 Desalination Publications. All rights reserved.

membranes by sol–gel technique, demonstrating anatase crystal structure. The induction of TiO_2 and combining PMR improved the dye removal efficiency to 82% compared to that of 65% by the membrane filtration alone. Mendret et al. [13] have studied the preparation of TiO_2 immobilized on flat-sheet alumina ceramic membrane by using a sol–gel. The experimental variables included layer coating, initial Acid Orange 7 concentration and pH. There were two main mechanisms for organic matter removal, including photodegradation and adsorption. In addition, higher photocatalytic activity was found at acidic pH (pH = 4) due to the higher adsorption. This indicated that pH had an influence on the organic matter removal mechanisms and that removal efficiency increased as photocatalytic activity increased. Wang et al. [14] have prepared TiO_2 catalyst immobilization on porous ceramic tubes by using a dip-coating technique and reported that the efficiency of the system increased with catalyst loading increased. In a study of humic acid removal by ceramic TiO_2-UF PMR, the parameters that affected PMR fouling included pH, crossflow velocities (CFV), and feed composition. A high CFV helped mitigating membrane fouling while changes in the permeate flux were related to TiO_2 loadings [15].

In addition, the PMR is able to use for microorganism removal/inactive or disinfection. Guo et al. [16] have studied TiO_2-photocatalytic membrane with coated outer surfaces for virus and bacteriophage P22 removal. Parallel experiments were performed for the alternative treatment of the turbid effluent. It found that hybrid TiO_2-coated membrane coupling with UV was high efficiency than other processes. The photocatalytic coating method was effective for the inhibition of virus removal and inactive by the turbidity. Jiang et al. [17] have studied PMR for the inactivation of bacteria from treated wastewater from the activated sludge process. The efficiency of microorganism removal is depending on the TiO_2 particle dosing that induced the adsorption mechanism on the TiO_2 surface before membrane rejection. Based on a literature review above, two key aspects that affect the performance of a photocatalytic membrane process are membrane preparation (materials, formulations, and techniques) and the operating conditions (flow rate, pH, initial concentration, etc.).

The use of organic chemical binders or additives in membrane ceramic synthesis can enhance the performance of the membrane-active layers [18]. The binder could penetrate into the membrane surface, obtained narrower retaining lines, enlarged the pores and increased ceramic density, thus induced higher flux [18,19]. Examples of various binders that were used to improve the properties of membranes in previous studies are polyvinylpyrrolidone [2,20], carboxymethyl cellulose [21], polyethylene glycol (PEG) [21,22], polyvinyl alcohol [23], sodium lauryl sulfate (SLS) [24], etc. Zhang et al. [22] used PEG as an additive and reported that increasing in PEG induced a larger pore size of the membrane. Boussemghoune et al. [25] had investigated different organic binders on ceramic support membrane and found that using PEG successfully enlarged the membrane pore size as confirmed by Brunauer–Emmett–Teller analysis. SLS is an anionic surfactant that is widely used for binding on polymeric or composite membranes [26]. SLS was used as a solution to disperse nanosized TiO_2 particles on the membrane surface, which resulted in membrane morphology improvement [27]. Even though using binder successfully improved pore size and TiO_2 particle distribution on the ceramic membrane, there is still a need to evaluate the effect of SLS and PEG binder on the ceramic photocatalytic membrane in an application where disinfection is needed.

In Thailand, activated sludge process, aerated lagoon and stabilized pond followed by chlorination for disinfection are commonly employed in hospital wastewater treatment plant (HWWTP). Even though the concentration of biochemical oxygen demand (BOD) and chemical oxygen demand (COD) in hospital wastewater are not high, the BOD/COD ratio was 0.64 and the total organic carbon (TOC) was approximately 223 mg/L [28]. Organic compounds are commonly found in the effluent of HWWTP and the reaction between these organic compounds and chemical disinfectants like chlorine can lead to the formation of harmful disinfection by-products (DBPs) including trihalomethanes (THMs). Jutaporn et al. [29] reported a significant correlation between THMs formation potential (THM-FP) and dissolved organic carbon (DOC). Hence, instead of chlorination, the photochemical reaction is proposed for hospital wastewater disinfection to minimize DBPs formation. Therefore, the objectives of this study are to evaluate the effects of binder in dip-coating of a ceramic membrane for PMR and to apply the coated ceramic membrane to remove organic compounds in treated wastewater effluent from hospitals.

2. Materials and methods

2.1. Preparation of ceramic membrane

The ceramic membrane was prepared from alumina (93 wt.%) and bentonite white (7 wt.%), by ball milling for 6 h, leaving in place for 1 d. The slip was then cast into a plaster mold. The tubular sample had a diameter, length and thickness for 50, 250 and 5 mm, respectively. The samples were then oven-dried at 110°C until the weight of the membrane samples became constant. Then the temperature was increased by 4.0°C/min until 1,100°C was reached. The samples were sintering at 1,100°C for 1 h, and then naturally cooled to a room temperature [30].

2.2. Deposition of photocatalytic coating on the membrane surface

TiO_2 powder (Sigma-Aldrich, Inc.) was used as a photocatalyst to coat on the lumen surface of the ceramic membrane. A mixture containing 10 wt.% of the catalyst was prepared by dissolving 100 g of TiO_2 powder into 900 g of Milli-Q water, then 0.02 g of SLS was added into the mixture as a dispersant. The suspension was stirred with a magnetic stirrer for 12 h and then sonicated in an ultrasonic bath for another 12 h. The dip-coating procedure using TiO_2 catalyst on the ceramic membrane was conducted according to Guo et al. [16]. The membrane coated with TiO_2 catalyst and SLS binder is referred to as TiO_2-SLS membrane. PEG was also used as a binder in the same dip-coating procedure, and the membrane prepared with TiO_2 catalyst and PEG is named TiO_2-PEG membrane.

2.3. Membrane characterization

The pore size of the membrane was determined using the mercury porosimetry method followed a procedure previously described by Huang et al. [31]. Morphological analyses of the non-coated membrane and the membrane coated with TiO_2 were conducted using scanning electron microscopy (SEM, TESCAN VEGA) to determine pore size, thickness and membrane structure. Crystal structure and phase composition of the membranes were characterized using X-ray diffraction (XRD) technique with Cu Ka wavelength and angle (2θ) of diffraction was varied from 20° to 70° (XRD, JSM-7600F diffractometer).

2.4. Sample collection and organic matter characterization

Treated wastewater effluent was collected from the two hospital wastewater treatment plants prior to chlorination. The first WWTP is an aerated lagoon (AL) locating in a private hospital, while the second WWTP is an activated sludge (AS) treatment plant locating in a public hospital. COD, pH, total suspended solids (TSS), and turbidity were analyzed following the Standard Method [32]. DOC was analyzed by TOC Analyzer (Multi N/C 3100, Germany). Dissolved organic matter (DOM) in the samples was characterized using the fluorescent excitation-emission matrix (EEM) (FP-8200, JASCO, Japan). EEM contour plots were visually inspected and the peak-picking method [33] was employed to determine the relative abundance of DOM fractions in the samples before and after treatment with PMR. EEMs were collected at excitation wavelengths from 200 to 500 nm at 5 nm increment and emission wavelengths from 210 to 550 nm at 5 nm increment. Four distinctive EEM peaks were observed at different excitation/emission (ex/em) coordinates, including tyrosine-like peak B (230/340 nm), tryptophan-like peak T (275/340 nm), terrestrial fulvic-like peak A (250 nm/420 nm), and terrestrial humic-like peak C (345/420 nm) [33,34]. Sample EEMs were subtracted with blank EEM of Milli-Q water, 1st and 2nd order Rayleigh masking, and then normalized to 1 using the highest value across all EEMs [35].

2.5. Evaluation of TiO_2 photocatalytic membrane performance

For a PMR batch experiment, the membrane was fully submerged in 1 L of wastewater effluent and then was placed under UV irradiation inside the membrane as shown in Fig. 1. The flow rate of the system was controlled at 120 mL/min by a peristaltic pump (Masterflex, USA). The pressure of the system was determined by a pressure sensor (Lutron MPS-384SD, Taiwan) directly connected to a personal computer.

The membrane permeate was collected in a beaker and the weight of the permeate was measured using a digital balance (AND, GF-3000, Japan) with an accuracy of ±0.1 g. Permeation flux (J, L/m² h or LMH) was calculated using the following equation:

$$J = \frac{M}{A\Delta t} \quad (1)$$

where M is the mass of permeate (L), A is the effective membrane area (m²), and Δt is the permeation time (h). COD and DOC removal efficiencies were calculated as follows:

$$\%\text{Removal} = \frac{\text{feed} - \text{permeate}}{\text{feed}} \text{value} \times 100 \quad (2)$$

where the feed and permeate correspond to the COD or DOC of the feed and permeate solutions, respectively.

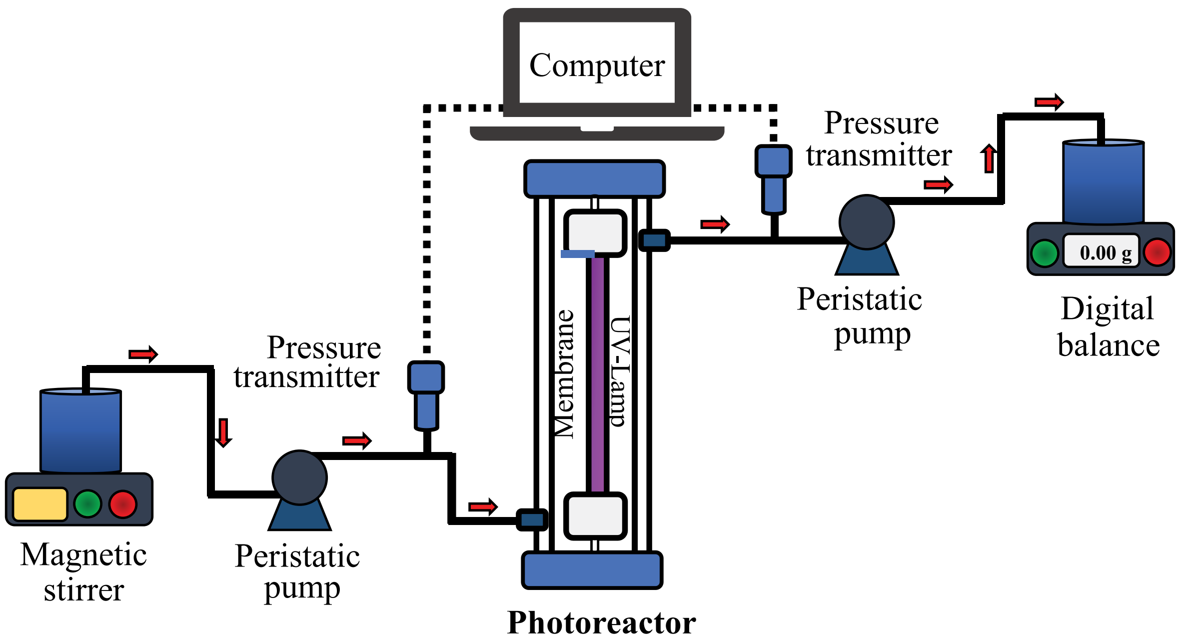

Fig. 1. Diagram of the experiment set-up.

The collected permeate samples were analyzed for pH, TSS, turbidity, COD, DOC, and fluorescent EEM.

3. Results and discussion

3.1. Membrane characteristics

The inner layer and cross-section images of the membrane obtained from SEM analysis are shown in Fig. 2. The ceramic membrane has a separation layer with 0.8 μm nominal pore size at the inner side of the membrane tube. SEM morphological analysis showed that, with TiO_2-coating, the membrane surfaces were smoother. The membrane thickness, including the intermediate and the top layers, is approximately 10.5 and 11 μm for TiO_2-SLS and TiO_2-PEG membranes, respectively. With TiO_2 dip-coating technique and hydroxyethyl cellulose organic binder, 3 μm layer of TiO_2 was reported in a previous study [36]. Thus, the cycles of the coating had a major effect on the thickness of the top layers. The lumen side of the TiO_2-SLS membrane is compacted and the top layer is separated distinctively compared to that in the TiO_2-PEG membrane (Fig. 2b and c). Moreover, the mass increase of the membranes was 5.39 and 3.37 g for TiO_2-SLS and TiO_2-PEG membranes, respectively, which suggesting that SLS was a more effective binder for the dip-coating technique.

XRD spectra were used to determine the elemental composition of the membranes (Fig. 3). The non-coated ceramic membrane composed of 49.3% aluminum (Al), 49.5% oxygen (O) and 1.2% calcium (Ca) (Fig. 3a). There was no significant difference of Ti components observed between the XRD spectra of TiO_2-SLS and TiO_2-PEG membranes. However, for the TiO_2-SLS membrane, silica (Si) was presented by 3%. This observation agreed well with the results from a previous study [12] reporting that the addition of 20%–33% silica into the photocatalytic membrane could suppress the phase transformation of TiO_2 from anatase to rutile. Hence, enhance the generation of hydroxyl radicals ($^{\bullet}OH$) for DOM oxidation [37]. This property of the TiO_2-SLS membrane could enhance its removal efficiency. Based on these membrane characterization results, it can be assumed that the TiO_2-SLS membrane would have greater removal efficiency compared to the TiO_2-PEG membranes.

3.2. Wastewater characteristics

The characteristics of the two treated wastewaters used in this study are presented in Table 1. Despite the higher turbidity of AS effluent, the two effluent samples had similar TSS concentrations. AS effluent had lower COD and DOC than AL effluent.

3.3. Membrane flux

Fig. 4a and b show the permeate flux obtained from the PMR experiments using AL effluent and AS effluent as feed solutions, respectively. For the PMR experiment using AL effluent as the feed, the initial flux of the non-coated, TiO_2-SLS and TiO_2-PEG membranes were 180, 179, and 133 LMH, respectively. Similarly, for the experiment using AS effluent, the initial flux of TiO_2-PEG membranes was lower than the other two membranes.

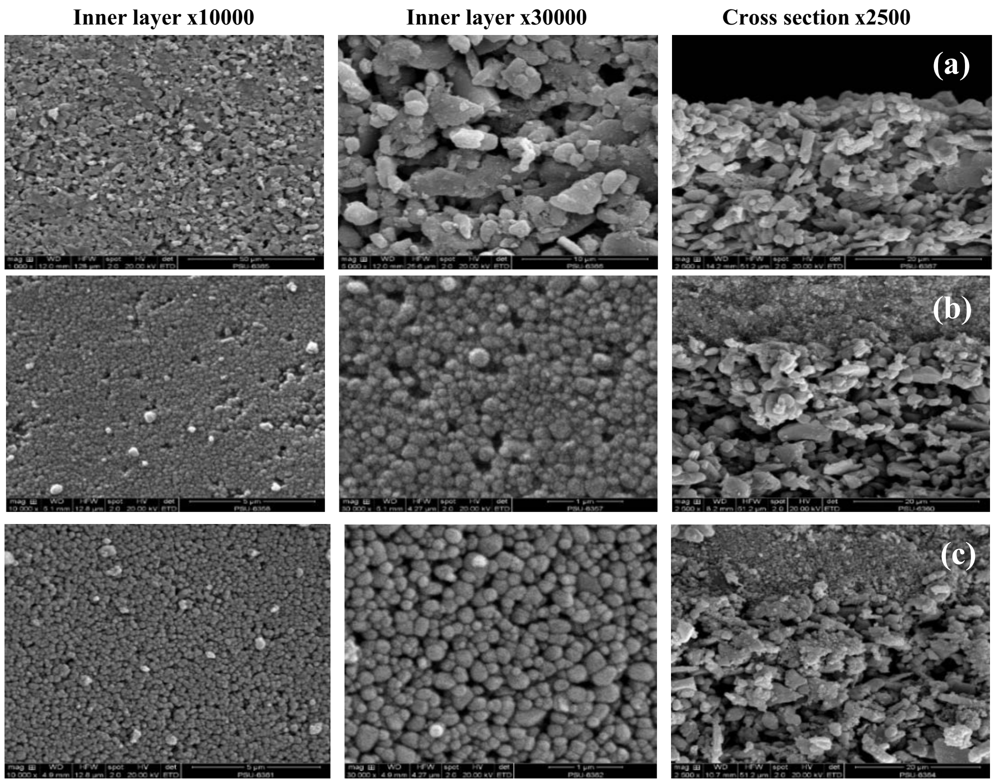

Fig. 2. SEM images of the ceramic membranes; (a) non-coated membrane, (b) TiO_2-SLS membrane, and (c) TiO_2-PEG membrane.

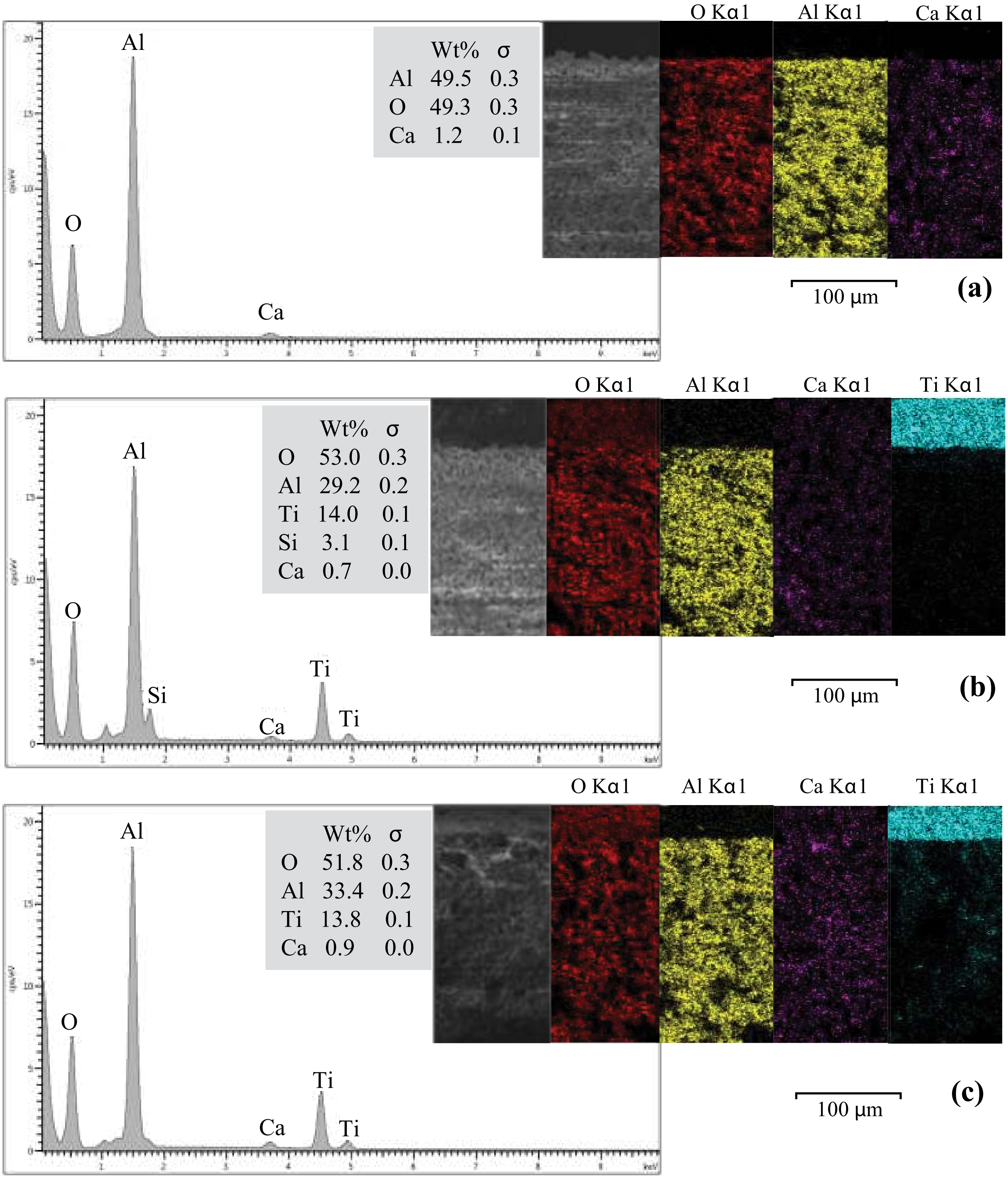

Fig. 3. XRD spectra of (a) non-coated membrane, (b) TiO_2-SLS membrane, and (c) TiO_2-PEG membrane.

The membrane resistance (R_m) was calculated according to Khongnakorn et al. [38], and R_m of the non-coated, TiO_2-SLS and TiO_2-PEG membranes were 5.49 × 10^{12}, 5.94 × 10^{12} and 6.25 × 10^{12} m^{-1}, respectively. Thus, the greater thickness (Fig. 2c) and the Ti dispensed in the inner surface of the TiO_2-PEG membrane (Fig. 3c) results in the greater R_m and subsequently less initial flux. Bu et al. [39] previously reported that PEG molecule can be exothermically adsorbed onto a TiO_2 oligomer through hydrogen bond formation. However, it seems that the step of coating in each cycle was also important to hydrophilicity/hydrophobicity of the top layer formed, thus affect membrane resistance.

After 30 min of PMR experiments, flux declined occurred 53%–69% for the non-coated membrane. While flux declined in the experiments using TiO_2-SLS and TiO_2-PEG membranes were in the range of 43%–74% and 60%–68%, respectively. The least flux decline (43%) was observed on the TiO_2-SLS membrane experiment using AS effluent.

3.4. Performance of the PMRs

3.4.1. Feed and permeate qualities

The operational conditions of the PMR experiment were kept constant with the flow rate of 120 mL/min and the temperature of 30°C for 30 min. The quality of feed and permeate water from the experiments are shown in Fig. 5. After 30 min of operation of the three types of PMR experiments, turbidity of the wastewater was drastically decreased in the range of 93%–97%. The permeate turbidity from the experiments using AL and AS effluent was 0.781.36 NTU and 1.10–1.14 NTU, respectively. These results show great turbidity removal efficiency of the PMR, which could be applied to treated secondary effluent to achieve better water quality.

For the experiments with AL effluent, COD removals by the non-coated, TiO_2-SLS and TiO_2-PEG membranes were 58%, 82% and 77%, respectively. For AS effluent, the COD removals by these three membranes were 56%, 78% and 61%. Thus, for the two water sources, the TiO_2-SLS membrane achieved the highest COD removal efficiency. Similarly, for DOC removal, PMR with TiO_2-SLS membrane achieved the highest removal of 32% and 25% for AL and AS effluent, respectively. While the treatment with the non-coated and the TiO_2-PEG membrane results in only 12%–28% DOC removal. Therefore, similar trends were observed in COD and DOC removals and that the highest removal occurred in the experiments with the TiO_2-SLS membrane.

Overall, these results have promising commercialization possibilities in applying the PMRs to treat secondary effluent for a non-portable water reuse application. The PMR with the TiO_2-SLS membrane showed the highest organic matter removal. Based on the membrane

Table 1
Characteristic of treated wastewater collected from two hospitals

Water quality parameter	AL effluent	AS effluent
pH	8.6	6.7
TSS (mg/L)	30	30
Turbidity (NTU)	20	43
COD (mg/L)	160	127
DOC (mg/L)	12.8	11.8

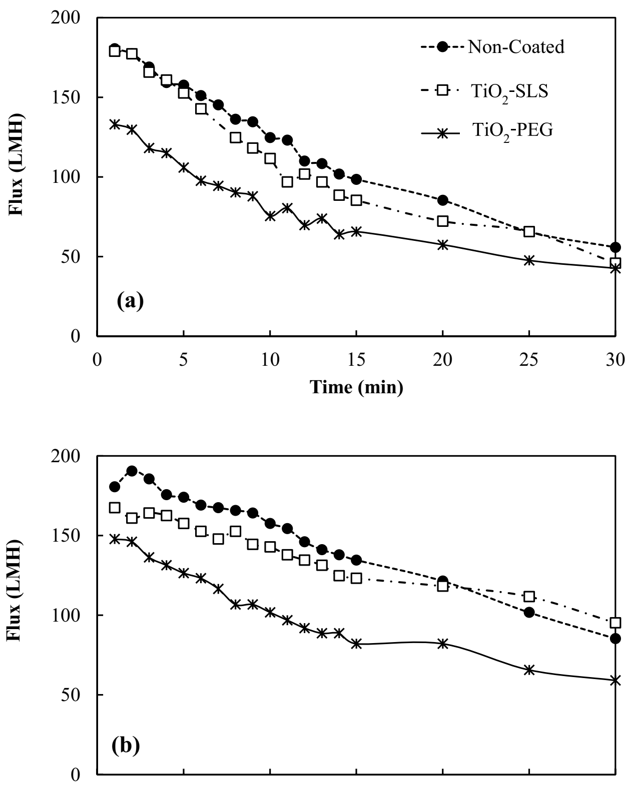

Fig. 4. Flux of the non-coated, TiO_2-SLS and TiO_2-PEG ceramic membranes obtained from the PMR experiments using (a) aerated lagoon effluent and (b) activated sludge effluent as feed solutions.

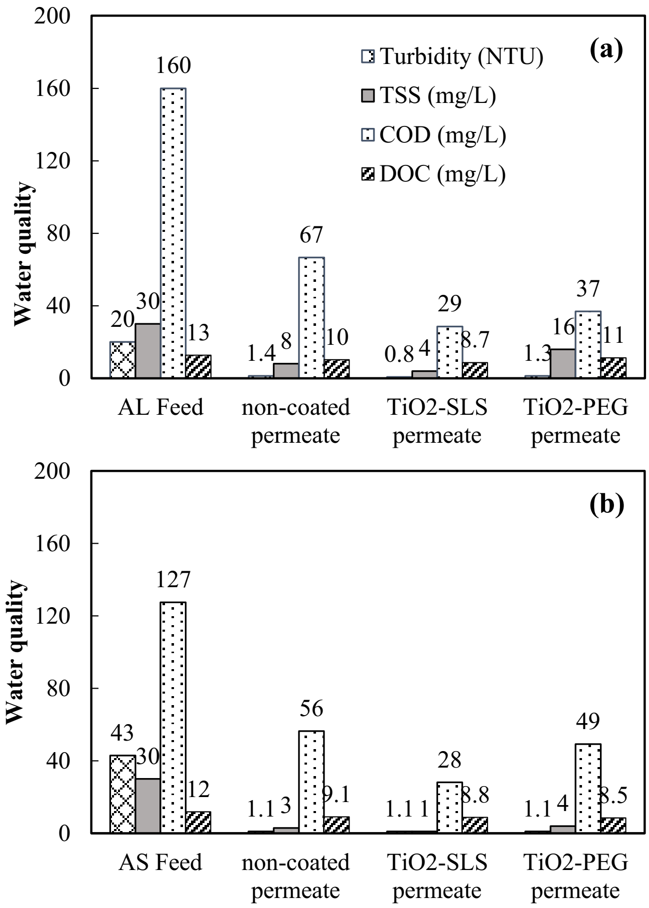

Fig. 5. Feed and permeate quality of the PMR experiments conducted using (a) aerated lagoon and (b) activated sludge as feed water. The operation condition; Q = 120 mL/min; t = 30 min; temperature = 30°C.

characterization results, the high efficiency of the TiO_2-SLS membrane was due to the presence of Si elements in the membrane structure and the increase of TiO_2 mass in the membrane. The deposition of TiO_2 on top of the membrane surface could also maximize the illumination of a light source to the surface of TiO_2, which could increase the photocatalytic activity.

3.4.2. DOM characterization using EEM

In this study, two feed and four permeate samples were collected from the experiments using coated membranes for DOM characterization using EEM analysis. A representative EEM contour plot obtained for the AL effluent feed water is shown in Fig. 6a. Based on the peak picking method [33], the EEM contour indicates that the main DOM presented in the AL effluent was humic-like and fulvic-like DOM (peaks C and A). Protein-like DOM, including tryptophan-like DOM (peak T) and tyrosine-like DOM (component T), also presented in the sample but their normalized fluorescent intensities were lower than those of humic and fulvic peaks. The presence of humic and fulvic-like DOM in AS system was contributed to their low biodegradability and the release of EPS from flocs [40].

After treatment with PMR-PEG (Fig. 6b), fluorescent intensities of the four peaks decrease noticeably by the chance in color scale. For a quantitative comparison, the fluorescence intensity at peaks A, B, C and T for all feed and permeate water is presented in Fig. 6c. Compared to AS effluent, AL effluent had lower fluorescent intensity at protein-like peaks B and T, but the higher intensity at peak C. This result could be explained by the lower concentration of microorganisms in the AL and also the ability of AL to remove tyrosine-like and tryptophan-like DOM [41].

For the experiments using TiO_2-PEG membrane, the PMRs exhibited good removal of protein-like DOM (peak B and T, 6.8%–22%) for both AS and AL feed water. For AL feed water, great removal of humic-like DOM (peak C, 29%) was also observed. However, an increase in fluorescent intensity of humic and fulvic DOM (peak C and A) in the range of (14%–41%) was observed after PMR treatment. This phenomenon could be explained by the generation of humic-like DOM caused by the photocatalytic degradation of protein-like DOM [42]. It is possible that a membrane treatment had preferential removal of protein-like DOM, and the breakdown of protein-like DOM could generate humic-like DOM, as a previous study [43] reported that permeate from membrane bioreactor contained predominantly humic-like DOM.

For the experiments using TiO_2-SLS membrane, the greatest fluorescent loss at peak B (40%) was observed in the case of AS effluent feed water. The reduction of fluorescent intensity at peak T was moderate (7.7%–27%). An increase in fulvic-like peak A (22%–34%) was also observed, similar to the experiments using TiO_2-PEG membrane. Overall, the PMRs exhibited preferential removal of protein-like DOM over humic and fulvic-like DOM, which agrees well with a previous study [42] reporting that the rate of photocatalytic degradation of protein-like DOM was found to be greater than that of humic-like DOM. During the photocatalytic reaction in the PMR, the protein-like DOM could be directly and preferably oxidized by the hydroxyl radicals in the solution. However, the breakdown of protein-like DOM by photocatalytic reaction could also lead to an increase in fluorescent intensity of humic-like DOM.

Previously, humic-like DOM was associated with the formation of carbonaceous DBPs [19,34], while protein-like DOM was previously associated with bacteria re-growth in distribution systems [44] and membrane fouling [45]. Hence, the greater removal of peak B and T suggests that the TiO_2-assisted PMR could be useful for membrane fouling reduction and prevention of bacterial re-growth in

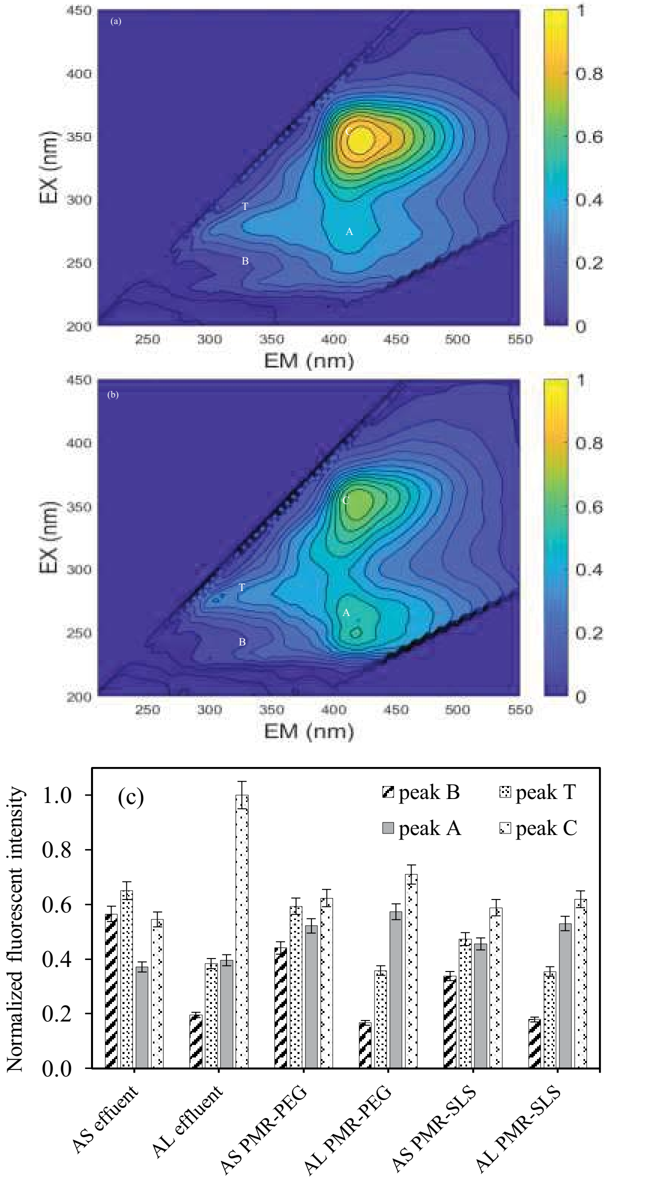

Fig. 6. Fluorescence excitation-emission matrices (EEMs) for (a) aerated lagoon effluent and (b) aerated lagoon effluent treated with PMR-PEG. (c) Normalized fluorescent intensities at peak A, B, C, and T. All data is normalized based on the highest peak value across all EEMs.

pipelines, but treatment for DBPs precursor removal might not be beneficial as much from the TiO_2-assisted PMR.

4. Conclusions

SLS and PEG were used as the binder in the synthesis of TiO_2 photocatalytic membrane for treatment of secondary effluent from the two hospitals. The PMR treatment with TiO_2-SLS membrane resulted in the highest COD removal and also moderate removal of DOC and fluorescent intensity of protein-like DOM. The main factors enhancing the performance of the TiO_2-SLS membrane were the presence of silica at the membrane surface and the formation of TiO_2 at the top layer for which increase photocatalytic activity. EEM characterization revealed that the TiO_2-assisted PMR had preferential removal of protein-like DOM over humic-like substances, as protein-like DOM was preferably oxidized by hydroxyl radicals in the reactor. Hence, the TiO_2-assisted PMR could be useful as a treatment for membrane fouling reduction and prevention of bacterial re-growth in pipelines.

Acknowledgments

The authors would like to acknowledges the support from the Center of Excellence in Membrane Science and Technology, Prince of Songkla University, Thailand. We also thank our collaborators at Songkhlanakarin hospital and Hatyai Hospital, Songkhla, Thailand, who facilitated water samples collection.

References

[1] C.P. Athanasekou, N.G. Moustakas, S. Morales-Torres, L.M. Pastrana-Martínez, J.L. Figueiredo, J.L. Faria, A.M.T. Silva, J.M. Dona-Rodriguez, G. Em. Romanos, P. Falaras, Ceramic photocatalytic membranes for water filtration under UV and visible light, Appl. Catal., B, 178 (2015) 12–19.

[2] R. Ahmad, C.S. Lee, J.H. Kim, J. Kim, Partially coated TiO_2 on Al_2O_3 membrane for high water flux and photodegradation by novel filtration strategy in photocatalytic membrane reactors, Chem. Eng. Res. Des., 163 (2020) 138–148.

[3] A. Golshenas, Z. Sadeghian, S.N. Ashrafizadeh, Performance evaluation of a ceramic-based photocatalytic membrane reactor for treatment of oily wastewater, J. Water Process Eng., 36 (2020) 101186, doi: 10.1016/j.jwpe.2020.101186.

[4] N. Turkten, Z. Cinar, A. Tomruk, M. Bekbolet, Copper-doped TiO_2 photocatalysts: application to drinking water by humic matter degradation, Environ. Sci. Pollut. Res., 26 (2019) 36096–36106.

[5] M. Bekbolet, S. Sen-Kavurmaci, The effect of photocatalytic oxidation on molecular size distribution profiles of humic acid, Photochem. Photobiol. Sci., 14 (2015) 576–582.

[6] R. Rajeswari, S. Kanmani, A study on synergistic effect of photocatalytic ozonation for carbaryl degradation, Desalination, 242 (2009) 277–285.

[7] Q. Li, R. Jia, J. Shao, Y. He, Photocatalytic degradation of amoxicillin via TiO_2 nanoparticle coupling with a novel submerged porous ceramic membrane reactor, J. Cleaner Prod., 209 (2019) 755–761.

[8] V.C. Sarasidis, K.V. Plakas, S.I. Patsios, A.J. Karabelas, Investigation of diclofenac degradation in a continuous photocatalytic membrane reactor. Influence of operating parameters, Chem. Eng. J., 239 (2014) 299–311.

[9] S. Leong, A. Razmjou, K. Wang, K. Hapgood, X. Zhang, H. Wang, TiO_2 based photocatalytic membranes: a review, J. Membr. Sci., 472 (2014) 167–184.

[10] E. Bet-Moushoul, Y. Mansourpanah, Kh. Farhadi, M. Tabatabaei, TiO_2 nanocomposite based polymeric membranes: a review on performance improvement for various applications in chemical engineering processes, Chem. Eng. J., 283 (2016) 29–46.

[11] I. Horovitz, V. Gitis, D. Avisar, H. Mamane, Ceramic-based photocatalytic membrane reactors for water treatment – where to next?, Rev. Chem. Eng., 36 (2020) 593–622.

[12] H. Zhang, X. Quan, S. Chen, H. Zhao, Y. Zhao, Fabrication of photocatalytic membrane and evaluation its efficiency in removal of organic pollutants from water, Sep. Purif. Technol., 50 (2006) 147–155.

[13] J. Mendret, M.H. Fraile, M. Rivallin, S. Brosillon, Hydrophilic composite membranes for simultaneous separation and photocatalytic degradation of organic pollutants, Sep. Purif. Technol., 111 (2013) 9–19.

[14] W.-Y. Wang, A. Irawan, Y. Ku, Photocatalytic degradation of Acid Red 4 using a titanium dioxide membrane supported on a porous ceramic tube, Water Res., 42 (2008) 4725–4732.

[15] K. Szymański, A.W. Morawski, S. Mozia, Humic acids removal in a photocatalytic membrane reactor with a ceramic UF membrane, Chem. Eng. J., 305 (2016) 19–27.

[16] B. Guo, E.V. Pasco, I. Xagoraraki, V.V. Tarabara, Virus removal and inactivation in a hybrid microfiltration-UV process with a photocatalytic membrane, Sep. Purif. Technol., 149 (2015) 245–254.

[17] L. Jiang, X. Zhang, K.H. Choo, Submerged microfiltration-catalysis hybrid reactor treatment: photocatalytic inactivation of bacteria in secondary wastewater effluent, Sep. Purif. Technol., 198 (2018) 87–92.

[18] Z. Chen, Z. Li, J. Li, C. Liu, C. Lao, Y. Fu, C. Liu, Y. Li, P. Wang, Y. He, 3D printing of ceramics: a review, J. Eur. Ceram. Soc., 39 (2019) 661–687.

[19] J. Moon, J.E. Grau, V. Knezevic, M.J. Cima, E.M. Sachs, Ink-jet printing of binders for ceramic components, J. Am. Ceram. Soc., 85 (2002) 755–762.

[20] K. Sirirerkratana, P. Kemacheevakul, S. Chuangchote, Color removal from wastewater by photocatalytic process using titanium dioxide-coated glass, ceramic tile, and stainless steel sheets, J. Cleaner Prod., 215 (2019) 123–130.

[21] H.R. Mahdavi, M. Arzani, T. Mohammadi, Synthesis, characterization and performance evaluation of an optimized ceramic membrane with physical separation and photocatalytic degradation capabilities, Ceram. Int., 44 (2018) 10281–10292.

[22] H. Zhang, X. Quan, S. Chen, H. Zhao, Y. Zhao, W. Li, Zirconia and titania composite membranes for liquid phase separation: preparation and characterization, Desalination, 190 (2006) 172–180.

[23] H. Wu, X. Xu, L. Shi, Y. Yin, L.-C. Zhang, Z. Wu, X. Duan, S. Wang, H. Sun, Manganese oxide integrated catalytic ceramic membrane for degradation of organic pollutants using sulfate radicals, Water Res., 167 (2019) 115110, doi: 10.1016/j.watres.2019.115110.

[24] T.A. Otitoju, P. Ugochukwu Okoye, G. Chen, Y. Li, M.O. Okoye, S. Li, Advanced ceramic components: materials, fabrication, and applications, J. Ind. Eng. Chem., 85 (2020) 34–65.

[25] N. Boussemghoune, M. Chikhi, Y. Ozay, P. Guler, B.O. Unal, N. Dizge, The investigation of organic binder effect on morphological structure of ceramic membrane support, Symmetry, 12 (2020) 770, doi: 10.3390/sym12050770.

[26] A.Y. Pulyalina, V. Rostovtseva, I. Faykov, A. Toikka, Application of polymer membranes for a purification of fuel oxygenated additive. Methanol/methyl tert-butyl ether (MTBE) separation via pervaporation: a comprehensive review, Polymers, 12 (2020) 2218, doi: 10.3390/polym12102218.

[27] Y. Yang, H. Zhang, P. Wang, Q. Zheng, J. Li, The influence of nano-sized TiO_2 fillers on the morphologies and properties of PSF UF membrane, J. Membr. Sci., 288 (2007) 231–238.

[28] A. Majumder, A.K. Gupta, P.S. Ghosal, M. Varma, A review on hospital wastewater treatment: a special emphasis on occurrence and removal of pharmaceutically active compounds, resistant microorganisms, and SARS-CoV-2, J. Environ. Chem. Eng., 9 (2021) 104812, doi: 10.1016/j.jece.2020.104812.

[29] P. Jutaporn, W. Laolertworakul, M.D. Armstrong, O. Coronell, Fluorescence spectroscopy for assessing trihalomethane precursors removal by MIEX resin, Water Sci. Technol., 79 (2019) 820–832.
[30] B. Darunee, T. Bhongsuwan, Slip casting of alumina for membrane application, J. Appl. Membr. Sci. Technol., 6 (2007) 35–43.
[31] C.Y. Huang, C.C. Ko, L.H. Chen, C.T. Huang, K.L. Tung, Y.C. Liao, A simple coating method to prepare superhydrophobic layers on ceramic alumina for vacuum membrane distillation, Sep. Purif. Technol., 198 (2018) 79–86.
[32] APHA, AWWA, WEF, Standard Methods for the Examination of Water and Wastewater, 22nd ed., American Public Health Association, American Water Works Association, Water Environment Federation, USA, 2012.
[33] P.G. Coble, Characterization of marine and terrestrial DOM in seawater using excitation-emission matrix spectroscopy, Mar. Chem., 51 (1996) 325–346.
[34] C.A. Stedmon, S. Markager, R. Bro, Tracing dissolved organic matter in aquatic environments using a new approach to fluorescence spectroscopy, Mar. Chem., 82 (2003) 239–254.
[35] Y. Engelborghs, A.J.W.G. Visser, Fluorescence Spectroscopy and Microscopy: Methods and Protocols, Methods in Molecular Biology, Vol. 1076, Springer, Switzerland, 2014, pp. 3–27.
[36] L. Djafer, A. Ayral, A. Ouagued, Robust synthesis and performance of a titania-based ultrafiltration membrane with photocatalytic properties, Sep. Purif. Technol., 75 (2010) 198–203.
[37] M. Antonopoulou, C. Kosma, T. Albanis, I. Konstantinou, An overview of homogeneous and heterogeneous photocatalysis applications for the removal of pharmaceutical compounds from real or synthetic hospital wastewaters under lab or pilot scale, Sci. Total Environ., 765 (2021) 144163, doi: 10.1016/j.scitotenv.2020.144163.
[38] W. Khongnakorn, W. Bootluck, P. Jutaporn, Surface modification of FO membrane by plasma-grafting polymerization to minimize protein fouling, J. Water Process Eng., 38 (2020) 101633, doi: 10.1016/j.jwpe.2020.101633.
[39] S. Bu, Z. Jin, X. Liu, H. Du, Z. Cheng, Preparation and formation mechanism of porous TiO_2 films using PEG and alcohol solvent as double-templates, J. Sol-Gel Sci. Technol., 30 (2004) 239–248.
[40] D. Mesquita, C. Quintelas, A. Amaral, E. Ferreira, Monitoring biological wastewater treatment processes: recent advances in spectroscopy applications, Rev. Environ. Sci. Biotechnol., 16 (2017) 395–424.
[41] C. Musikavong, S. Wattanachira, F. Nakajima, H. Furumai, Three dimensional fluorescent spectroscopy analysis for the evaluation of organic matter removal from industrial estate wastewater by stabilization ponds, Water Sci. Technol., 55 (2007) 201–210.
[42] D.D. Phong, J. Hur, Insight into photocatalytic degradation of dissolved organic matter in UVA/TiO_2 systems revealed by fluorescence EEM-PARAFAC, Water Res., 87 (2015) 119–126.
[43] K. Poojamnong, K. Tungsudjawong, W. Khongnakorn, P. Jutaporn, Characterization of reversible and irreversible foulants in membrane bioreactor (MBR) for eucalyptus pulp and paper mill wastewater treatment using fluorescence regional integration, J. Environ. Chem. Eng., 8 (2020) 104231, doi: 10.1016/j.jece.2020.104231.
[44] L. Yang, J. Hur, W. Zhuang, Occurrence and behaviors of fluorescence EEM-PARAFAC components in drinking water and wastewater treatment systems and their applications: a review, Environ. Sci. Pollut. Res., 22 (2015) 6500–6510.
[45] P. Jutaporn, P.C. Singer, R.M. Cory, O. Coronell, Minimization of short-term low-pressure membrane fouling using a magnetic ion exchange (MIEX®) resin, Water Res., 98 (2016) 225–234.